

AD-A183 308

NMR DSC DMA AND HIGH PRESSURE ELECTRICAL CONDUCTIVITY  
STUDIES IN PPO COMP (U) HUNTER COLL NEW YORK DEPT OF  
PHYSICS AND ASRRONOMY J J FONTANELLA ET AL 01 JUL 87

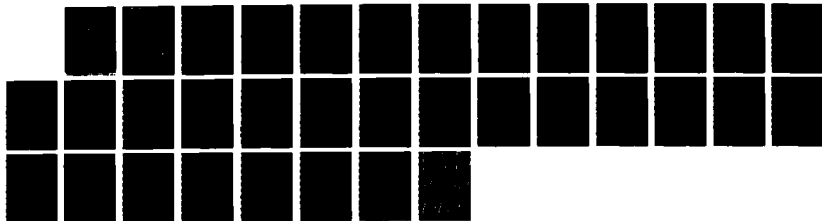
1/1

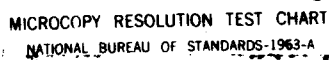
UNCLASSIFIED

TR-26 N00014-87-AF-0001

F/G 7/4

NL





MICROCOPY RESOLUTION TEST CHART  
NATIONAL BUREAU OF STANDARDS-1963-A

12

AD-A183 308

OFFICE OF NAVAL RESEARCH

Contract N00014-87-AF-00001

R&T Code 413d001—02

Technical Report No. 26

NMR, DSC, DMA, and High Pressure Electrical Conductivity Studies in  
PPO Complexed with Sodium Perchlorate

by

John J. Fontanella & Mary C. Wintersgill

Prepared for Publication

in the

Journal of the Electrochemical Society

U. S. Naval Academy  
Department of Physics  
Annapolis, MD 21402-5026

July 1, 1987

SECRET  
JUL 31 1987  
A

Reproduction in whole or in part is permitted for  
any purpose of the United States Government

\* This document has been approved for public release  
and sale; its distribution is unlimited

Unclassified

SECURITY CLASSIFICATION OF THIS PAGE

## REPORT DOCUMENTATION PAGE

1a. REPORT SECURITY CLASSIFICATION Unclassified			1b. RESTRICTIVE MARKINGS		
2a. SECURITY CLASSIFICATION AUTHORITY			3. DISTRIBUTION / AVAILABILITY OF REPORT This document has been approved for public release and sale; its distribution is unlimited.		
2b. DECLASSIFICATION / DOWNGRADING SCHEDULE			5. MONITORING ORGANIZATION REPORT NUMBER(S)		
4. PERFORMING ORGANIZATION REPORT NUMBER(S) 26					
6a. NAME OF PERFORMING ORGANIZATION U. S. Naval Academy		6b. OFFICE SYMBOL (if applicable)		7a. NAME OF MONITORING ORGANIZATION	
6c. ADDRESS (City, State, and ZIP Code) Physics Department Annapolis, MD 21402-5026			7b. ADDRESS (City, State, and ZIP Code)		
8a. NAME OF FUNDING / SPONSORING ORGANIZATION Office of Naval Research		8b. OFFICE SYMBOL (if applicable)		9. PROCUREMENT INSTRUMENT IDENTIFICATION NUMBER	
8c. ADDRESS (City, State, and ZIP Code) 800 N. Quincy Street Arlington, VA 22217-5000			10. SOURCE OF FUNDING NUMBERS		
			PROGRAM ELEMENT NO. 61153N	PROJECT NO. RR013-06-0C	TASK NO. 627-793
11. TITLE (Include Security Classification) NMR, DSC, DMA, and High Pressure Electrical Conductivity Studies in PPO Complexed with Sodium Perchlorate (Unclassified)					
12. PERSONAL AUTHOR(S) John J. Fontanella and Mary C. Wintersgill					
13a. TYPE OF REPORT Interim		13b. TIME COVERED FROM 86/10/1 TO 87/9/30		14. DATE OF REPORT (Year, Month, Day) 1987 July 1	
15. PAGE COUNT 25					
16. SUPPLEMENTARY NOTATION					
17. COSATI CODES			18. SUBJECT TERMS (Continue on reverse if necessary and identify by block number)		
FIELD	GROUP	SUB-GROUP	Prepared for publication in the Journal of the Electrochemical Society		
19. ABSTRACT (Continue on reverse if necessary and identify by block number)					
<p>Audio frequency electrical conductivity, DSC, DMA, and <sup>23</sup>Na NMR measurements have been carried out on Parel 58 elastomer complexed with sodium perchlorate. (As Parel 58 is primarily poly(propylene oxide), it will be referred to as PPO.) The DSC and DMA measurements yield similar values for T<sub>g</sub> which are about 72°C higher than the "central" T<sub>g</sub> for uncomplexed PPO. In addition, the DSC studies show that the sodium perchlorate is insoluble above about 140°C. The conductivity measurements have been carried out in vacuum over the temperature range 290-380K and at pressures up to 0.65 GPa from 315-370K. From a VTF analysis E<sub>a</sub> is found to be about 0.09 eV and T<sub>g</sub> is found to be about 45°C below the "central" glass transition temperature which is the same behavior observed</p>					
20. DISTRIBUTION / AVAILABILITY OF ABSTRACT <input checked="" type="checkbox"/> UNCLASSIFIED/UNLIMITED <input type="checkbox"/> SAME AS RPT <input type="checkbox"/> DTIC USERS			21. ABSTRACT SECURITY CLASSIFICATION Unclassified		
22a. NAME OF RESPONSIBLE INDIVIDUAL John J. Fontanella			22b. TELEPHONE (Include Area Code) 301-267-3487		22c. OFFICE SYMBOL

*cont'd* → 19. previously for PPO complexed with lithium salts and for the alpha relaxation in uncomplexed material. In addition, it is found that the vacuum activation volumes for the electrical conductivity and the alpha relaxation are approximately the same when compared relative to  $T_0$ . The  $^{23}\text{Na}$  NMR measurements reveal the presence of both bound and mobile sodium species, the relative concentrations of which change by about a factor of ten over the temperature range  $-90$  to  $+90^\circ\text{C}$ . In addition the mobile  $^{23}\text{Na}$  resonance becomes motionally narrowed above  $T_g$ . The NMR results combined with the conductivity data imply that ion motion is controlled by large scale segmental motions of the polymer chains. ↑

Accession For	
GRA&I	<input checked="checked" type="checkbox"/>
DAIC TAB	<input type="checkbox"/>
Unannounced	<input type="checkbox"/>
Justification	
By	
Distribution/	
Availability Codes	
Avail and/or	
Special	
A-1	



NMR, DSC, DMA, AND HIGH PRESSURE ELECTRICAL CONDUCTIVITY STUDIES IN PPO  
COMPLEXED WITH SODIUM PERCHLORATE\*

S. G. Greenbaum and Y. S. Pak

Physics Department  
Hunter College of CUNY  
New York, NY 10021

M. C. Wintersgill, J. J. Fontanella, and J. W. Schultz

Physics Department  
U. S. Naval Academy  
Annapolis, MD 21402

C. G. Andeen

Physics Department  
Case Western Reserve University  
Cleveland, OH 44106

# ABSTRACT

Audio frequency electrical conductivity, DSC, DMA, and  $^{23}\text{Na}$  NMR measurements have been carried out on Parel 58 elastomer complexed with sodium perchlorate. (As Parel 58 is primarily poly(propylene oxide), it will be referred to as PPO.) The DSC and DMA measurements yield similar values for  $T_g$  which are about  $72^\circ\text{C}$  higher than the "central"  $T_g$  for uncomplexed PPO. In addition, the DSC studies show that the sodium perchlorate is insoluble above about  $140^\circ\text{C}$ . The conductivity measurements have been carried out in vacuum over the temperature range 290-380K and at pressures up to 0.65 GPa from 315-370K. From a VTF analysis  $E_a$  is found to be about 0.09 eV and  $T_0$  is found to be about  $45^\circ\text{C}$  below the "central" glass transition temperature which is the same behavior observed previously for PPO complexed with lithium salts and for the  $\alpha$  relaxation in uncomplexed material. In addition, it is found that the vacuum activation volumes for the electrical conductivity and the  $\alpha$  relaxation are approximately the same when compared relative to  $T_0$ . The  $^{23}\text{Na}$  NMR measurements reveal the presence of both bound and mobile sodium species, the relative concentrations of which change by about a factor of ten over the temperature range  $-90$  to  $+90^\circ\text{C}$ . In addition the mobile  $^{23}\text{Na}$  resonance becomes motionally narrowed above  $T_g$ . The NMR results combined with the conductivity data imply that ion motion is controlled by large scale segmental motions of the polymer chains.

## INTRODUCTION

In recent papers, results for the temperature and pressure variation of electrical conductivity in PPO complexed with lithium salts along with the temperature and pressure variation of the  $\alpha$  relaxation have been presented.<sup>1,2</sup> The most important result of that work is that it was shown that to within experimental uncertainty, the temperature and pressure variation of the electrical conductivity was found to be the same as the temperature and pressure variation of the electrical relaxation time for the  $\alpha$  relaxation. This provides quantitative evidence that, for PPO, ionic conductivity is controlled by large-scale segmental motions (conformational rearrangements of the polymer chain backbone<sup>3</sup>) characteristic of the glass-rubber transition. "Such rearrangements occur by a mechanism of hindered rotation around main chain bonds and involve cooperative thermal motions of individual chain segments. The hindrance to these 'micro-Brownian' motions can be described in terms of viscous or frictional forces which result from interactions of the moving segment with neighboring molecules or with segments within the same chain."<sup>3</sup> However, in the earlier paper,<sup>2</sup> it was emphasized that the conductivity results alone could not be used to elucidate the transport mechanism as the shift in carrier concentration with temperature was unknown. In the present paper both electrical conductivity and nuclear magnetic resonance (NMR) measurements are carried out on PPO complexed with sodium perchlorate. The combination of the results provides strong evidence that the large scale segmental motions control ion motion. Also, DSC and DMA studies are reported for the same material.



## EXPERIMENTAL

The techniques for performing audio frequency complex impedance/electrical relaxation measurements over a wide range of temperatures and pressures are given elsewhere.<sup>1</sup> The key element in the measurements is a CGA-82 microprocessor-controlled bridge operating at seventeen frequencies from  $10\text{-}10^5$  Hz. Once again, the material studied was Parel 58 (Hercules, Inc.) elastomer which is a sulfur-vulcanizable copolymer of propylene oxide and allyl glycidyl ether. As the material is approximately 95% propylene oxide, it is referred to as PPO. Samples were obtained by solution casting using methanol as the solvent. The materials were dried at about  $110^\circ\text{C}$  under vacuum continuously provided by an Alcatel 2008 pump. All procedures including loading of the samples into the various sample holders were carried out in a dry box with a relative humidity of less than 5%.

In the present work, gold electrodes were vacuum evaporated onto the surfaces of the material in either a three-terminal or two-terminal configuration. The samples were about 1 mm thick and the electrodes about 4 mm in diameter.

The differential scanning calorimetry (DSC) studies were carried out using a DuPont 910 DSC controlled by a DuPont 990 console which was interfaced with an Apple II+ microcomputer. The dynamic mechanical analysis studies (DMA) were carried out using a DuPont 982 DMA controlled by another modified DuPont 990 console.

The  $^{23}\text{Na}$  NMR measurements were performed at 81 MHz utilizing standard pulse techniques. Good signal-to-noise ratios were obtainable by

averaging 500-1000 free induction decays (FID's). Linewidths and relative intensities of the two resolvable lineshape components were extracted from the FID's by selective saturation and subtraction as discussed later. Temperatures were controlled to within  $\pm 2^{\circ}\text{C}$  by a nitrogen flow system.

## RESULTS

### Thermal Analysis

The DSC results for  $\text{PPO}_8\text{NaClO}_4$  are shown in Fig. 1. Results for uncomplexed PPO are included for comparison. It is clear that the complexed material is highly amorphous in that it exhibits a strong glass transition with a "central"  $T_g$  of about 283K (The "onset"  $T_g$  is about 278K and the "end" is at about 288K.) Consequently,  $T_g$  is about  $72^{\circ}\text{C}$  higher than for the uncomplexed material for which the "central" glass transition temperature is about 211K.<sup>1</sup> Similar results were obtained via DMA studies as seen in Fig. 2. An increase in  $T_g$  with the addition of salt to PPO is a well known phenomenon.<sup>4</sup>

In addition, in the DSC studies for  $\text{PPO}_8\text{NaClO}_4$ , a strong endothermic event is observed at about  $140^{\circ}\text{C}$ . In order to obtain information concerning this feature, the material was annealed at various temperatures, quenched to  $-150^{\circ}\text{C}$  as rapidly as possible in situ, and the DSC studies repeated. Typical results for the quenched material after anneal at temperatures above  $140^{\circ}\text{C}$  are shown in Fig. 1c. In all cases, a strong glass transition typical of uncomplexed PPO is observed. In addition, there is a broad feature centered at about  $-20^{\circ}\text{C}$  and a high temperature exothermic event followed by an endotherm. It is to be emphasized that such behavior was not observed for quenched material annealed below  $140^{\circ}\text{C}$ ,

all data being similar to Fig. 1b. Consequently, it is concluded that at about 140°C the salt comes out of solution. Support for this interpretation can be found in the work of Teeters and Frech<sup>5</sup> who observed a finely divided crystalline solid in PPO-NaSCN above 165°C and showed that the Raman spectrum was the same as microcrystalline NaSCN. Electrical conductivity studies would be of interest, however, for the materials discussed so far the temperature at which salt precipitation occurs is outside the range of the present equipment. However, the authors have recently shown that for PPO<sub>8</sub>NaI and PPO<sub>8</sub>KSCN salt precipitation DSC endotherms are observed at 100°C and 60°C respectively.<sup>6</sup> In both cases, the electrical conductivity follows VTF or WLF behavior (see the discussion below) for temperatures somewhat below the salt precipitation temperature, then becomes significantly less than the expected value as temperature increases further. In addition, the <sup>23</sup>Na NMR studies in PPO<sub>8</sub>NaI show a drop in the ratio of the mobile to bound sodium ions at about the temperature of conductivity anomaly. Finally, the DSC studies for PPO<sub>8</sub>KSCN show behavior analogous to the results of the Raman studies of Teeters and Frech for PPO<sub>8</sub>NaSCN.<sup>5</sup> Specifically, DSC features similar to that observed for the pure salt are observed in the polymer after heating above the salt precipitation temperature.

#### NMR

The <sup>23</sup>Na NMR results for PPO<sub>8</sub>NaClO<sub>4</sub> bear a striking similarity to those obtained for cross-linked poly(dimethylsiloxane-ethylene oxide) (PDMS-EO) complexes with NaCF<sub>3</sub>COO.<sup>7,8</sup> An important feature common to both systems is the presence of two lineshape components throughout the

temperature range of about  $-100$  to  $+100^{\circ}\text{C}$ . In the PPO complex, the two  $^{23}\text{Na}$  are characterized by vastly different spin-lattice relaxation times ( $T_1$ ). The short- $T_1$  ( $\sim 0.2$ - $30$  ms) component is slightly narrower than the long- $T_1$  ( $\sim 1$ s) component at low temperatures, and undergoes substantial motional narrowing above  $T_g$ . The long  $T_1$  resonance, on the other hand, does not appear to have a pronounced temperature dependence until about  $75^{\circ}\text{C}$ , at which point broadening is observed. The short- $T_1$  narrow line is therefore attributed to mobile  $\text{Na}^+$  ions while a bound Na configuration gives rise to the broad line.

The two to three order of magnitude difference in  $T_1$ 's facilitated the acquisition of the separate lineshape components by selective saturation and subtraction. Free induction decays for the broad and narrow lines at two temperatures are shown in Fig. 3. Comparison of Figs. 3a ( $5^{\circ}\text{C}$ ) and 3b ( $35^{\circ}\text{C}$ ) highlights the temperature insensitivity of the broad line, while comparison of Figs. 3a and 3c demonstrates the similarity (except for their  $T_1$  values) between the broad and narrow lines just below  $T_g$ .

The ratio of the narrow line to broad line intensities (N/B) as a function of reciprocal temperature is plotted in Fig. 4. Perhaps the most crucial feature of the data in Fig. 4 is that the mobile ion concentration increases by only one order of magnitude over a temperature range in which the conductivity increases by five orders of magnitude. Therefore, carrier generation plays only a minor role in the conductivity mechanism. Comparison of Fig. 4 with conductivity data to be discussed later further highlights the relatively weak temperature dependence of the mobile  $\text{Na}^+$  generation. The small decrease in N/B observed at the higher temperature

end of the plot is not presently understood. Another phenomenon which merits further study is the observation of a transition from first to second-order quadrupole broadening of the bound Na resonance above about 75°C. A similar observation was noted in the PDMS/EO complex, although the latter transition occurs at about 25°C, and was attributed to the dissociation of ion triplets (i.e.  $\text{Na}_2\text{X}^+$  or  $\text{NaX}_2^-$ ) into neutral ion pairs and single ions.<sup>5</sup> However, this model conflicts with the above-mentioned high temperature decrease in N/B, unless the majority of the triplet species are  $\text{NaX}_2^-$ , whose dissociation would not yield additional  $\text{Na}^+$  ions. Therefore, the possibility that the broad resonance may be attributable to Na bonded to the polymer chains must be explored.

As deduced from temperature and pressure-dependent conductivity and dielectric loss measurements to be discussed later, the primary mechanism believed to drive the ionic conductivity is large scale segmental motion associated with the glass-rubber transition. Figure 5 is a plot of the mobile Na resonance linewidth (obtained by saturating the bound resonance) as a function of temperature. It is clear from the data that the onset of motional narrowing occurs in the vicinity of the glass transition temperature, again indicating the importance of polymer chain motion to ionic mobility. The increase in linewidth above 60°C is due to rapid spin-lattice relaxation ( $T_1 \leq 300 \mu\text{s}$ ) which introduces a lifetime broadening contribution to the total linewidth.

#### Electrical Conductivity

The techniques used to obtain values of the electric conductivity from complex impedance or admittance measurements are given elsewhere.<sup>1,2</sup>

The results of a typical vacuum data run are shown in Fig. 6. The curvature often observed for amorphous polymer systems is apparent. Consequently, the conductivity data were first analyzed via the VTF equation:<sup>9</sup>

$$\sigma = AT^{-1/2} \exp^{-[E_a/k(T-T_0)]} \quad (1)$$

with the adjustable parameters A,  $E_a$ , and  $T_0$ . A non-linear least squares fit of Eq. (3) to the data was carried out and the results are  $E_a=0.096$  eV,  $T_0=237.6$ K, and  $\log_{10}A((\Omega\text{-cm})^{-1}\sqrt{K})=0.71$ . The RMS deviation in  $\log_{10}\sigma$  was 0.012.

The vacuum value for  $T_0$  is about 45°C lower than the "central"  $T_g=283$ K which was determined by DSC and DMA. Similar results have also been recently reported for PPO complexed with lithium salts<sup>1,2</sup> and for poly(dimethyl siloxane-ethylene oxide) co-polymer containing a sodium salt.<sup>7,8</sup> This result is consistent with the configurational entropy model<sup>10,11</sup> where  $T_0$  is interpreted as the temperature of zero configurational entropy which would be expected to occur at a much lower temperature than DSC or DMA  $T_g$ 's.

Next, isothermal data (data taken at a fixed temperature and various pressures) were taken and typical results are similar to those shown elsewhere for PPO complexed with lithium salts.<sup>1,2</sup> A least squares fit of the following equation:

$$\log_{10}\sigma = \log_{10}\sigma_0 + aP + bP^2 \quad (2)$$

to the isothermal data was carried out and the resultant fitting parameters,  $\log_{10}\sigma_0$ ,  $a$ , and  $b$ , are listed in Table I. The data were used to determine activation volumes directly via:

$$\Delta V^* = -kT \, d \ln \sigma / dP \quad (3)$$

The vacuum values are also listed in Table I. The activation volumes for  $\text{PPO}_8\text{NaClO}_4$  and the previous results for PPO complexed with lithium salts<sup>1</sup> are plotted in Fig. 7 vs.  $T-T_0$ . The plot shows that the activation volume is approximately the same for all materials at a given temperature interval above  $T_0$ . Consequently, different vacuum activation volumes can merely be attributed to different  $T_0$ 's.

In addition, the activation volume associated with the electrical relaxation time for the  $\alpha$  relaxation was calculated from:

$$\Delta V^* = -kT \, d \ln \tau / dP \quad (4)$$

where  $\tau$  is the electrical relaxation time. The results are also plotted in Fig. 7. It is seen that to within the scatter in the data, on the "reduced plot" they are the same as those obtained from the electrical conductivity. This provides strong, albeit indirect evidence that electrical conductivity is controlled by the same mechanism as the  $\alpha$  relaxation. It has been known for many years that the  $\alpha$  relaxation is due to large scale segmental motions of the polymer chains.<sup>3</sup> Consequently, since the NMR results described above show that carrier generation plays only a minor role in electrical conductivity, the results show that ion

motion is controlled by large scale segmental motions of the polymer chains.

It is also noted that the activation volume calculated from Eq. (3) decreases as temperature increases. This agrees with previous observations in PEO<sup>12,13</sup>. Further, this is expected since in general activation volumes scale with activation energy and, as is apparent from Fig. 6, the activation energy (slope of the conductivity plot) clearly decreases as temperature increases.

Next, the data were analyzed in terms of the WLF equation:<sup>14</sup>

$$\log_{10} \frac{\sigma(T)}{\sigma(T_g)} = \frac{C_1(T-T_g)}{C_2+(T-T_g)} \quad (5)$$

The resultant parameters for  $T_g=283K$  are  $C_1=10.5$ ,  $C_2=44.7K$ , and  $\log_{10}[(\sigma(T_g)(\Omega\text{-cm})^{-1})]=-11.2$ . The RMS deviation was 0.01. The values of  $C_1$  and  $C_2$  are reasonably close to the "universal" values of 17.4 and 51.6K.<sup>15</sup>

Finally, for completeness, the data were analyzed via the mathematically equivalent VTF eq. in the form:

$$\sigma = A' \exp^{-[E'_a/k(T-T'_0)]} \quad (6)$$

The best-fit parameters are  $E'_a=0.093$  eV,  $T'_0=238.3K$ , and  $\log_{10}A'((\Omega\text{-cm})^{-1})=-0.66$ .

In previous papers, the authors have presented isobaric data or an isobaric analysis of isothermal data. In particular, high pressure VTF parameters were reported.<sup>1,2</sup> When that procedure was attempted for



$\text{PPO}_8\text{NaClO}_4$ , somewhat unusual results were obtained. Specifically, the best fit parameters for 0, 0.1, 0.2, and 0.3 GPa were  $E_a=0.096, 0.091, 0.10,$  and  $0.12$  eV, respectively, and  $T_o=238, 254, 263,$  and  $267\text{K}$ , respectively. The unusual feature, which is a decrease in  $E_a$  from 0.096 to 0.091 as pressure increases from "vacuum" to 0.1 GPa may possibly be attributable, in part, to the effect of high pressure on the solubility of the salt. Specifically, it was shown above from the DSC studies that the salt comes out of solution at high temperature. If pressure were to decrease the solubility at high temperatures, the high temperature, high pressure results would be strongly affected and thus anomalous high pressure VTF parameters would be expected. Further work concerning this point is necessary.

#### SUMMARY

In summary, then, the following results have been obtained:

- (a)  $^{23}\text{Na}$  NMR-determined mobile to bound sodium ratios exhibit a factor of ten increase over a temperature range ( $\sim -90$  to  $+90^\circ\text{C}$ ) in which the conductivity increases by five orders of magnitude. Thus carrier generation plays a relatively minor role in the transport mechanism. Motional narrowing of the mobile  $^{23}\text{Na}$  resonance is observed, with the onset of the narrowing occurring at  $T_g$ .
- (b) It has been found that the electrical conductivity in  $\text{PPO}_8\text{NaClO}_4$  exhibits the same pressure and temperature dependence as the relaxation time for the  $\alpha$  relaxation in uncomplexed PPO.
- (c) The combination of the NMR and electrical conductivity data provides evidence that ion motion is controlled by the large scale segmental motions of the polymer chains characteristic of the glass-rubber transition.

#### ACKNOWLEDGMENTS

The authors would like to thank Hercules, Inc. for supplying the Parel 58 elastomer. Ms. M. Chia is acknowledged for assistance with the NMR measurements and data analysis. This work was supported in part by the Office of Naval Research, and the PSC-CUNY Research Award Program.

# REFERENCES

1. J. J. Fontanella, M. C. Wintersgill, M. K. Smith, J. Semancik, and C. G. Andeen, J. Appl. Phys., 60, 2665 (1986).
2. J. J. Fontanella, M. C. Wintersgill, J. P. Calame, M. K. Smith, and C. G. Andeen, Solid State Ionics, 18&19, 253 (1986).
3. N. G. McCrum, B. E. Read, and G. Williams, Anelastic and Dielectric Effects in Polymeric Solids, (Wiley, New York, 1967).
4. J. Moacanin and E. F. Cuddihy, J. Polymer Science: Part C, 14, 313 (1966).
5. D. Teeters and R. Frech, Solid State Ionics, 18&19, 271 (1986).
6. M. C. Wintersgill, J. J. Fontanella, S. G. Greenbaum, and K. J. Adamic, Proceedings of the International Symposium on Polymer Electrolytes, St. Andrews, Scotland, 17-19 June 1987, to be published in the British Polymer Journal.
7. K. J. Adamic, S. G. Greenbaum, M. C. Wintersgill, and J. J. Fontanella, J. Appl. Phys., 60, 1342 (1986).
8. M. C. Wintersgill, J. J. Fontanella, M. K. Smith, S. G. Greenbaum, K. J. Adamic, and C. G. Andeen, Polymer, 28, 633 (1987).
9. H. Vogel, Physik Z., 22, 645 (1921); V.G. Tammann and W. Hesse, Z. Anorg. Allg. Chem., 156, 245 (1926); G.S. Fulcher, J. Am. Ceram. Soc., 8, 339 (1925).
10. J. H. Gibbs and E.A. DiMarzio, J. Chem. Phys. 28 (1958) 373.
11. G. Adam and J.H. Gibbs, J. Chem. Phys. 43 (1965) 139.
12. J. J. Fontanella, M. C. Wintersgill, J. P. Calame, F. P. Pursel, D. R. Figueroa, and C. G. Andeen, Solid State Ionics, 9&10, 1139 (1983).
13. A. V. Chadwick, J. H. Strange, and M. R. Worboys, Solid State Ionics

9&10, 1155 (1983).

14. M. L. Williams, R. F. Landel, and J. D. Ferry, J. Am. Chem. Soc., 77, 3701 (1955).

15. H. Schneider, M. Brekner, and H. Cantow, Polymer Bulletin, 14, 479 (1985).

Table 1. Best fit parameters in equation 4 and zero pressure activation volumes.

Maximum pressure (GPa)	T(K)	RMS Deviation	$\log_{10} \sigma_0$ $(\Omega\text{-cm})^{-1}$	$a(\text{GPa})^{-1}$	$b(\text{GPa})^{-2}$	$\Delta V^*$ $(\text{cm}^3/\text{mol})$
0.10	314.6	0.037	-6.833	-14.1	-18.0	84.7
0.21	319.1	0.0054	-6.485	-12.1	-17.5	73.8
0.25	328.6	0.0091	-5.875	-10.4	-10.0	65.5
0.33	338.2	0.040	-5.368	-7.97	-10.2	51.6
0.30	343.0	0.0093	-5.152	-7.48	-6.34	49.1
0.42	348.3	0.011	-4.938	-6.31	-7.71	42.1
0.53	363.8	0.011	-4.412	-5.32	-3.90	37.0
0.56	368.0	0.041	-4.288	-5.36	-3.73	37.7

#### FIGURE CAPTIONS

Figure 1. DSC plot for (a) uncomplexed PPO (b) as-prepared  $\text{PPO}_8\text{NaClO}_4$ , and (c)  $\text{PPO}_8\text{NaClO}_4$  after having been annealed above  $140^\circ\text{C}$ . The data were taken at 10 K/min. The data for (b) and (c) are for the same sample plotted on the same scale. However, the data for (a) has not been normalized for sample mass and thus only the temperatures associated with the event are meaningful, not its magnitude.

Figure 2. DMA plot for (a) uncomplexed PPO and (b) as-prepared  $\text{PPO}_8\text{NaClO}_4$ . The data were taken at 5 K/min.

Figure 3.  $^{23}\text{Na}$  free induction decays in  $\text{PPO}_8\text{NaClO}_4$ : (a) long- $T_1$  component at  $5^\circ\text{C}$  and (b)  $35^\circ\text{C}$  and the short- $T_1$  component at (c)  $5^\circ$  and (d)  $35^\circ\text{C}$ .

Figure 4. Reciprocal temperature plot of narrow to broad line intensity ratios in  $\text{PPO}_8\text{NaClO}_4$ .

Figure 5.  $^{23}\text{Na}$  linewidth of the mobile sodium obtained by saturating the bound sodium resonance. The onset of motional narrowing occurs at about  $T = T_g$ . The high temperature broadening is attributable to rapid spin-lattice relaxation.

Figure 6. Arrhenius plot of the electrical conductivity data. The squares represent the datum points and the solid line is the best fit VTF equation (equation 1).

Figure 7. Vacuum activation volumes vs. reduced temperature for (a) x-the electrical relaxation time for the  $\alpha$  relaxation from reference 1, (b) the electrical conductivity for: diamonds- $\text{PPO}_8\text{LiCF}_3\text{SO}_3$ , squares- $\text{PPO}_8\text{LiClO}_4$ ,  $\Delta$ - $\text{PPO}_8\text{LiI}$ ,  $\times$ - $\text{PPO}_8\text{LiSCN}$  from reference 1, and (c) pentagons- $\text{PPO}_8\text{NaClO}_4$ .

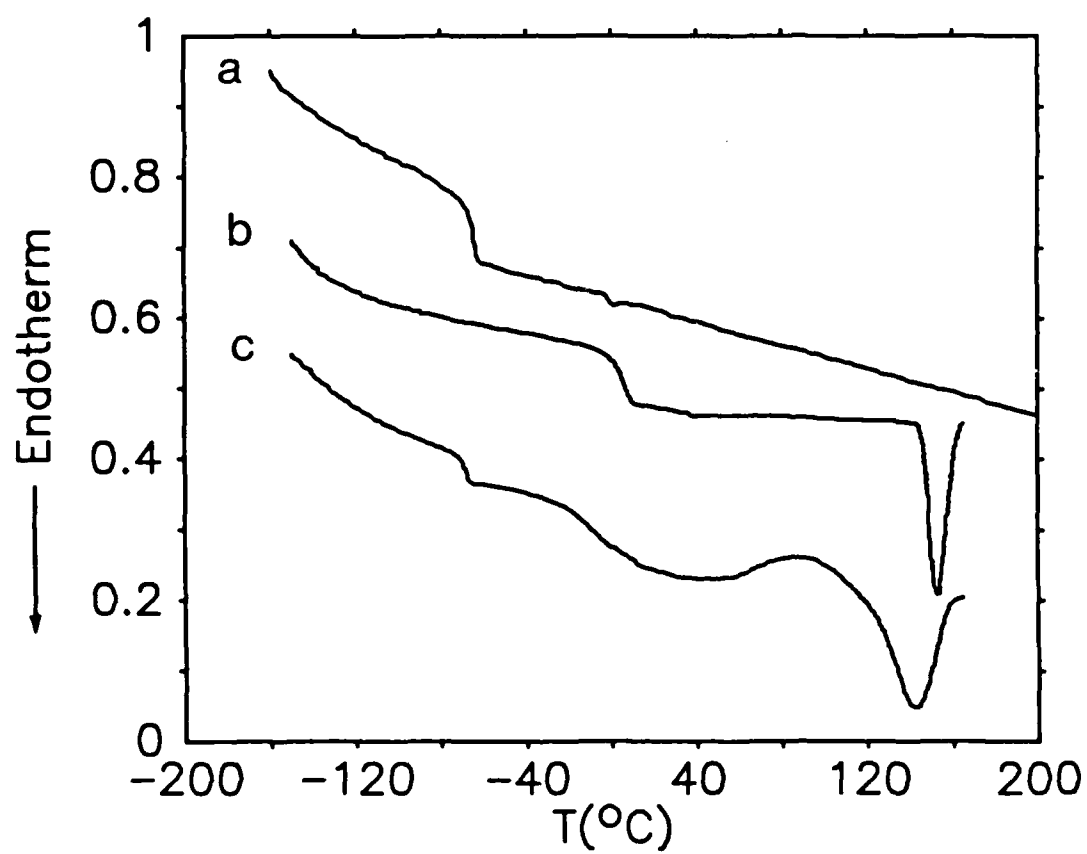


Figure 1



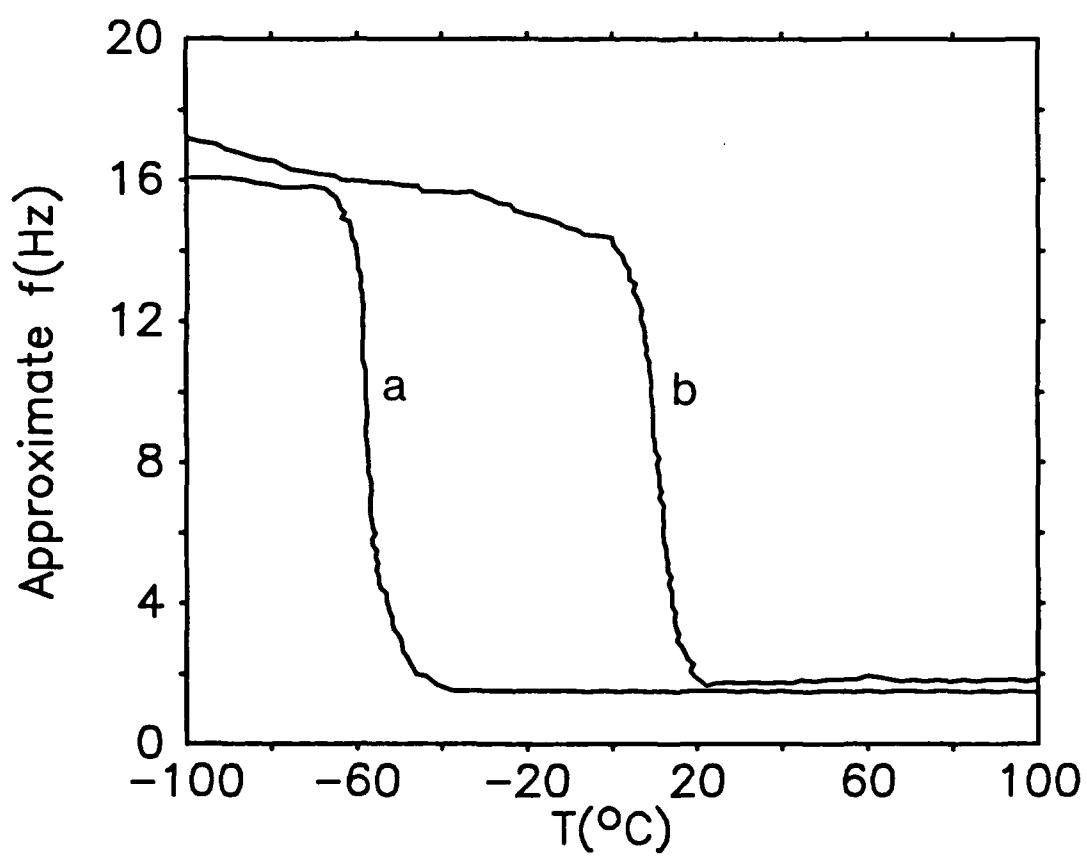


Figure 2

# $^{23}\text{Na}$ FID

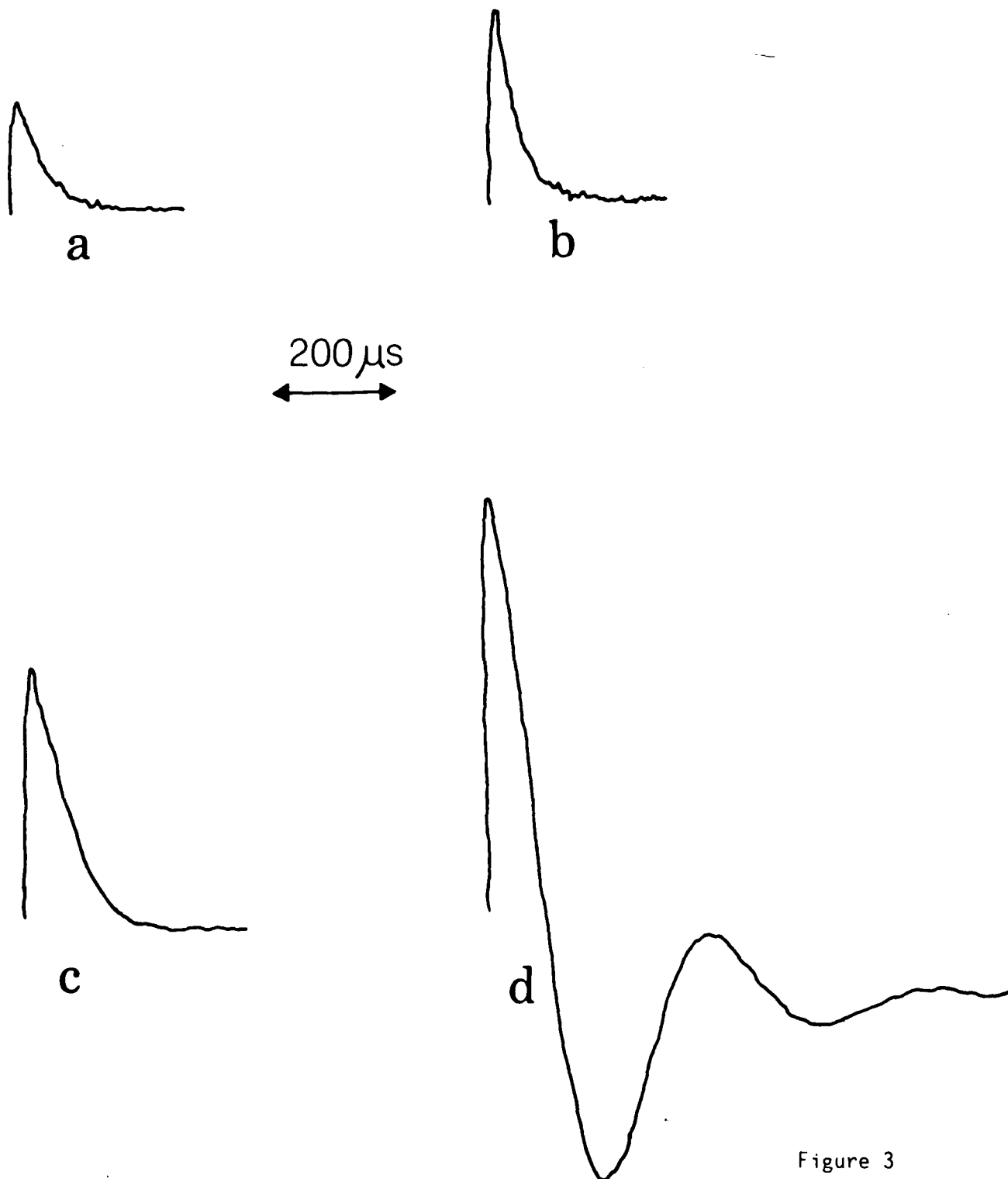


Figure 3

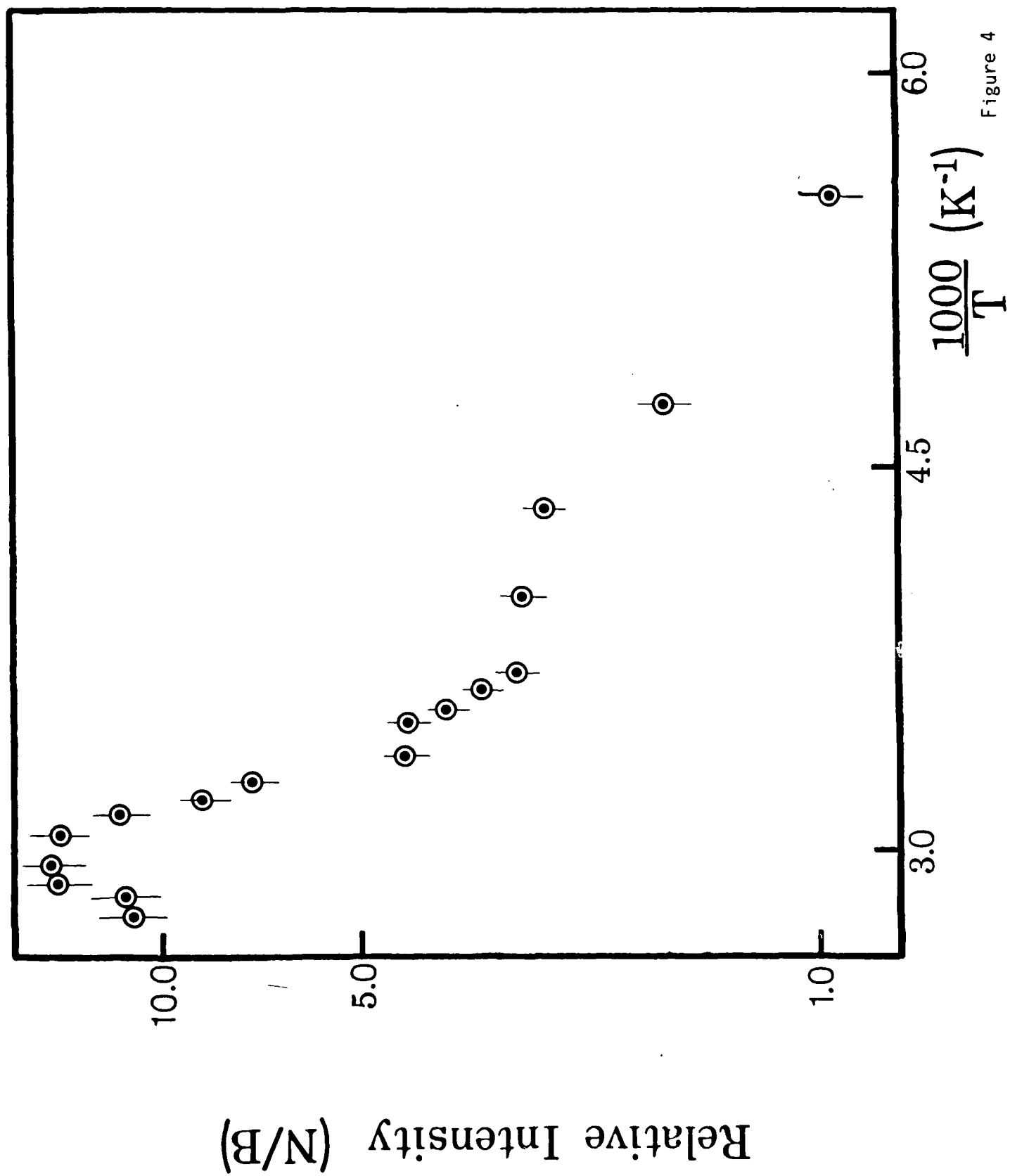


Figure 4

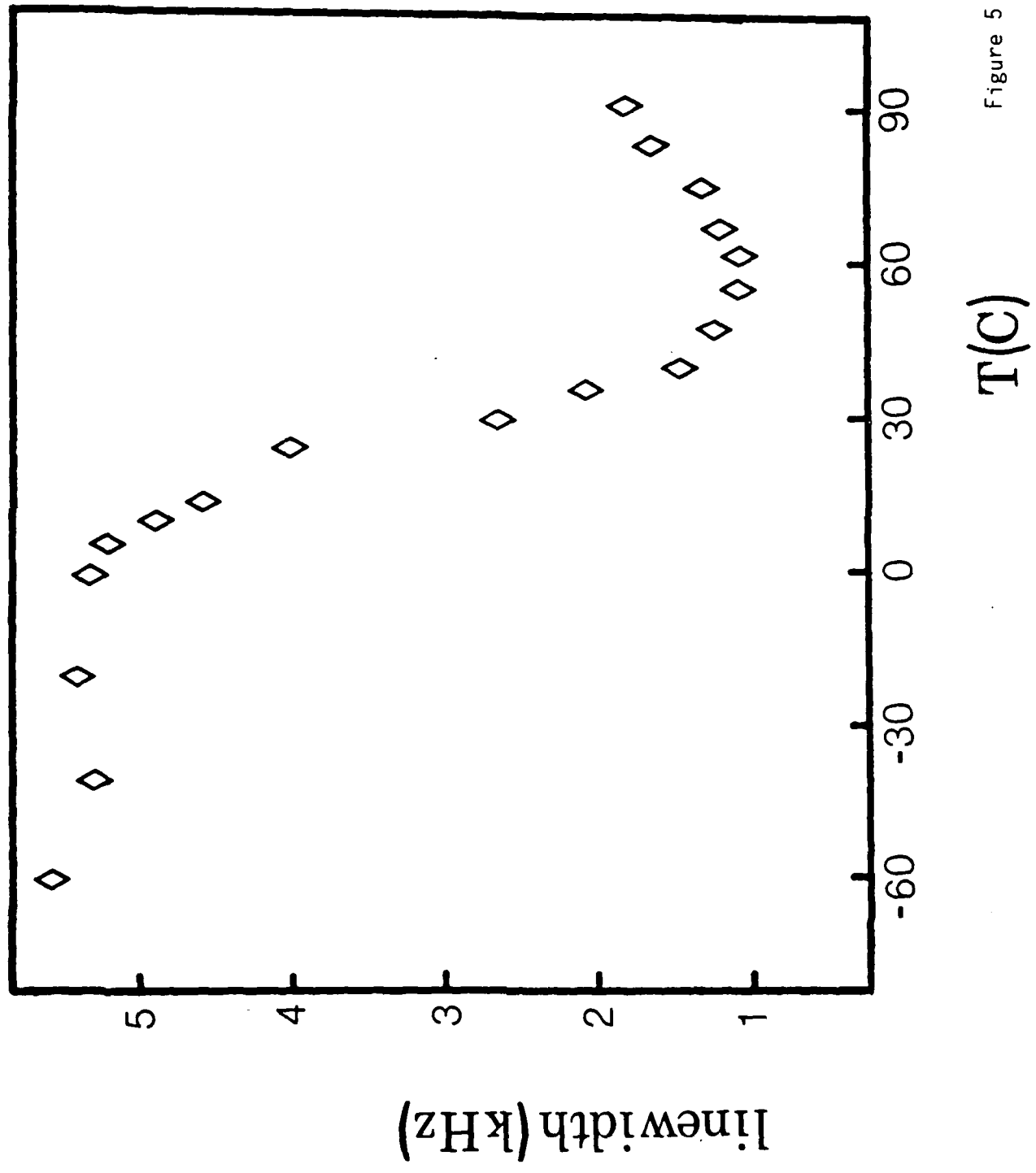


Figure 5

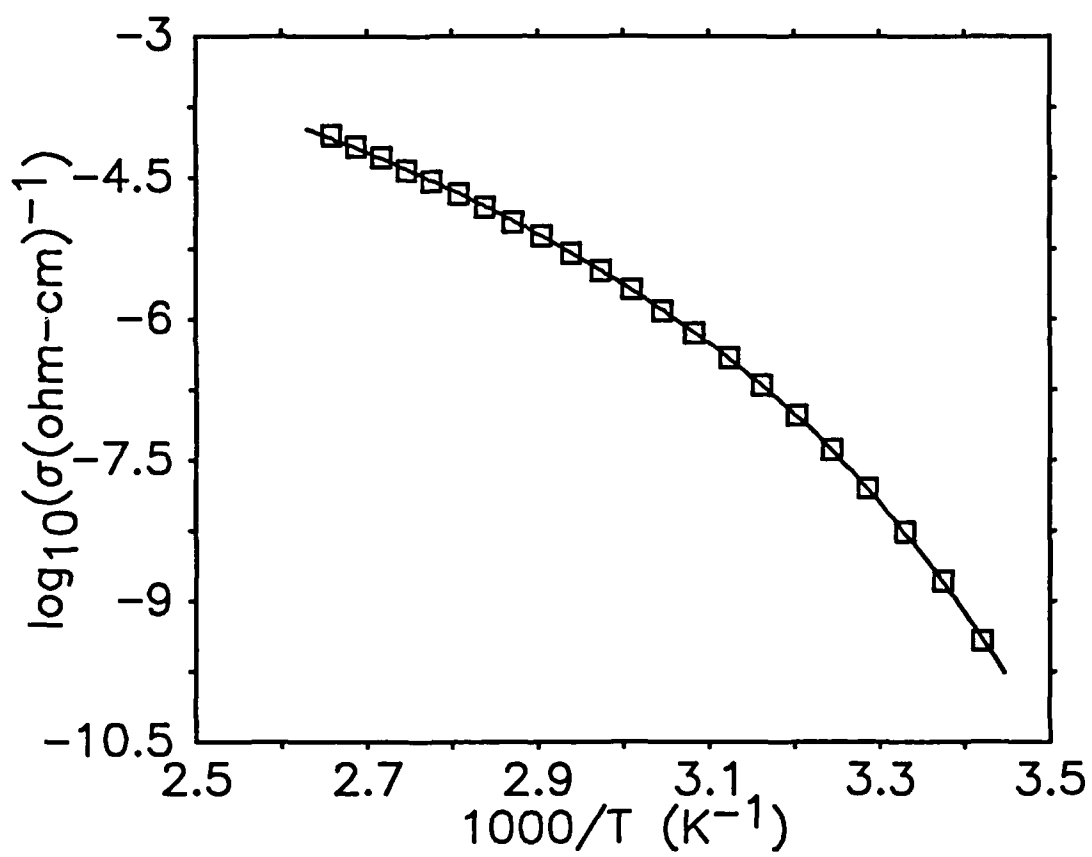


Figure 6

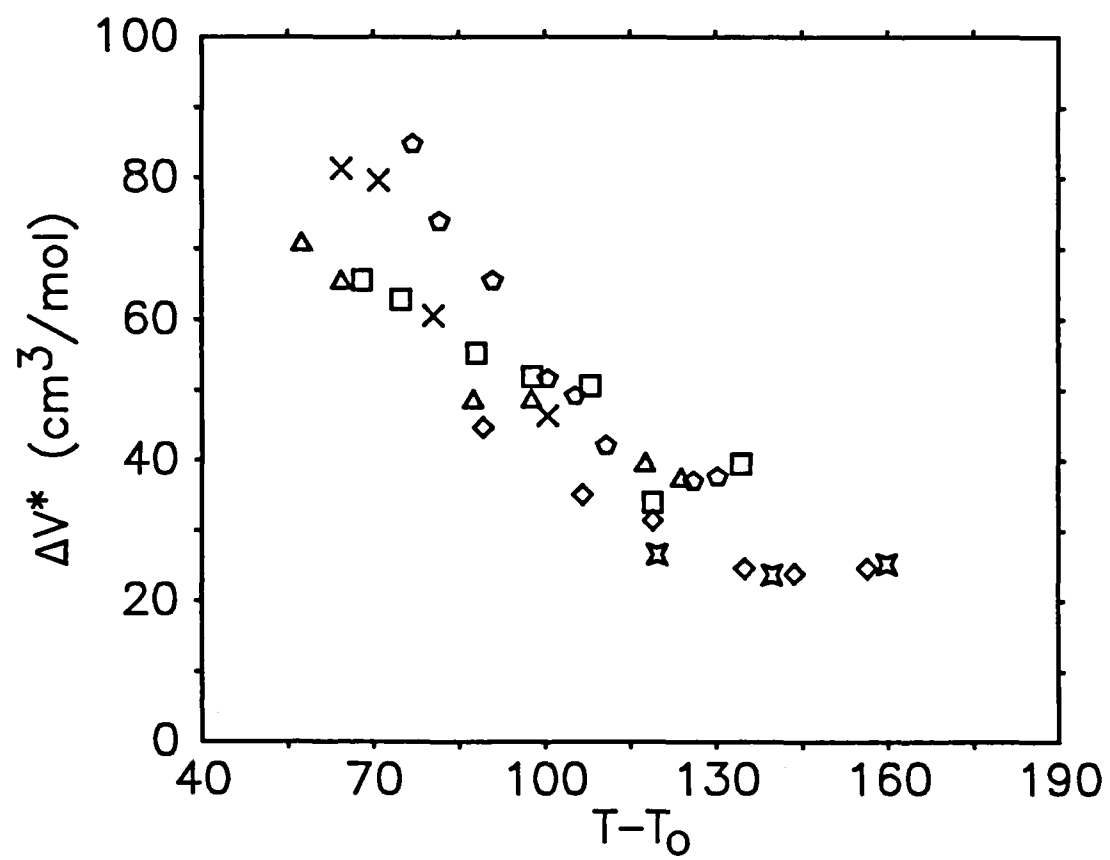


Figure 7

DL/1113/87/2

TECHNICAL REPORT DISTRIBUTION LIST, GEN

	<u>No. Copies</u>		<u>No. Copies</u>
Office of Naval Research Attn: Code 1113 800 N. Quincy Street Arlington, Virginia 22217-5000	2	Dr. David Young Code 334 NORDA NSTL, Mississippi 39529	1
Dr. Bernard Douda Naval Weapons Support Center Code 50C Crane, Indiana 47522-5050	1	Naval Weapons Center Attn: Dr. Ron Atkins Chemistry Division China Lake, California 93555	1
Naval Civil Engineering Laboratory Attn: Dr. R. W. Drisko, Code L52 Port Hueneme, California 93401	1	Scientific Advisor Commandant of the Marine Corps Code RD-1 Washington, D.C. 20380	1
Defense Technical Information Center Building 5, Cameron Station Alexandria, Virginia 22314	12 high quality	U.S. Army Research Office Attn: CRD-AA-IP P.O. Box 12211 Research Triangle Park, NC 27709	1
DTNSRDC Attn: Dr. H. Singerman Applied Chemistry Division Annapolis, Maryland 21401	1	Mr. John Boyle Materials Branch Naval Ship Engineering Center Philadelphia, Pennsylvania 19112	1
Dr. William Tolles Superintendent Chemistry Division, Code 6100 Naval Research Laboratory Washington, D.C. 20375-5000	1	Naval Ocean Systems Center Attn: Dr. S. Yamamoto Marine Sciences Division San Diego, California 91232	1

ABSTRACTS DISTRIBUTION LIST, 359/627

Dr. Manfred Breiter  
Institut für Technische Elektrochemie  
Technischen Universität Wien  
9 Getreidemarkt, 1160 Wien  
AUSTRIA

Dr. E. Yeager  
Department of Chemistry  
Case Western Reserve University  
Cleveland, Ohio 44106

Dr. R. Sutula  
The Electrochemistry Branch  
Naval Surface Weapons Center  
Silver Spring, Maryland 20910

Dr. R. A. Marcus  
Department of Chemistry  
California Institute of Technology  
Pasadena, California 91125

Dr. J. J. Auborn  
AT&T Bell Laboratories  
600 Mountain Avenue  
Murray Hill, New Jersey 07974

Dr. M. S. Wrighton  
Chemistry Department  
Massachusetts Institute  
of Technology  
Cambridge, Massachusetts 02139

Dr. B. Stanley Pons  
Department of Chemistry  
University of Utah  
Salt Lake City, Utah 84112

Dr. Bernard Spielvogel  
U.S. Army Research Office  
P.O. Box 12211  
Research Triangle Park, NC 27709

Dr. Mel Miles  
Code 3852  
Naval Weapons Center  
China Lake, California 93555

Dr. P. P. Schmidt  
Department of Chemistry  
Oakland University  
Rochester, Michigan 48063

Dr. Roger Belt  
Litton Industries Inc.  
Airtron Division  
Morris Plains, NJ 07950

Dr. Ulrich Stimming  
Department of Chemical Engineering  
Columbia University  
New York, NY 10027

Dr. Royce W. Murray  
Department of Chemistry  
University of North Carolina  
Chapel Hill, North Carolina 27514

Dr. Michael J. Weaver  
Department of Chemistry  
Purdue University  
West Lafayette, Indiana 47907

Dr. R. David Rauh  
EIC Laboratories, Inc.  
Norwood, Massachusetts 02062

Dr. Edward M. Eyring  
Department of Chemistry  
University of Utah  
Salt Lake City, UT 84112

Dr. M. M. Nicholson  
Electronics Research Center  
Rockwell International  
3370 Miraloma Avenue  
Anaheim, California

Dr. Nathan Lewis  
Department of Chemistry  
Stanford University  
Stanford, California 94305

Dr. Hector D. Abruna  
Department of Chemistry  
Cornell University  
Ithaca, New York 14853

Dr. A. B. P. Lever  
Chemistry Department  
York University  
Downsview, Ontario M3J 1P3



ABSTRACTS DISTRIBUTION LIST, 359/627

Dr. Martin Fleischmann  
Department of Chemistry  
University of Southampton  
Southampton SO9 5H UNITED KINGDOM

Dr. John Wilkes  
Department of the Air Force  
United States Air Force Academy  
Colorado Springs, Colorado 80840-6528

Dr. R. A. Osteryoung  
Department of Chemistry  
State University of New York  
Buffalo, New York 14214

Dr. Janet Osteryoung  
Department of Chemistry  
State University of New York  
Buffalo, New York 14214

Dr. A. J. Bard  
Department of Chemistry  
University of Texas  
Austin, Texas 78712

Dr. Steven Greenbaum  
Department of Physics and Astronomy  
Hunter College  
695 Park Avenue  
New York, New York 10021

Dr. Donald Sandstrom  
Boeing Aerospace Co.  
P.O. Box 3999  
Seattle, Washington 98124

Mr. James R. Moden  
Naval Underwater Systems Center  
Code 3632  
Newport, Rhode Island 02840

Dr. D. Rolison  
Naval Research Laboratory  
Code 6171  
Washington, D.C. 20375-5000

Dr. D. F. Shriver  
Department of Chemistry  
Northwestern University  
Evanston, Illinois 60201

Dr. Alan Bewick  
Department of Chemistry  
The University of Southampton  
Southampton, SO9 5NH UNITED KINGDOM

Dr. Edward Fletcher  
Department of Mechanical Engineering  
University of Minnesota  
Minneapolis, Minnesota 55455

Dr. Bruce Dunn  
Department of Engineering &  
Applied Science  
University of California  
Los Angeles, California 90024

Dr. Elton Cairns  
Energy & Environment Division  
Lawrence Berkeley Laboratory  
University of California  
Berkeley, California 94720

Dr. Richard Pollard  
Department of Chemical Engineering  
University of Houston  
Houston, Texas 77004

Dr. M. Philpott  
IBM Research Division  
Mail Stop K 33/801  
San Jose, California 95130-6099

Dr. Martha Greenblatt  
Department of Chemistry, P.O. Box 939  
Rutgers University  
Piscataway, New Jersey 08855-0939

Dr. Anthony Sammells  
Eltron Research Inc.  
4260 Westbrook Drive, Suite 111  
Aurora, Illinois 60505

Dr. C. A. Angell  
Department of Chemistry  
Purdue University  
West Lafayette, Indiana 47907

Dr. Thomas Davis  
Polymers Division  
National Bureau of Standards  
Gaithersburg, Maryland 20899

ABSTRACTS DISTRIBUTION LIST, 359/627

Dr. Stanislaw Szpak  
Naval Ocean Systems Center  
Code 633, Bayside  
San Diego, California 95152

Dr. Gregory Farrington  
Department of Materials Science  
and Engineering  
University of Pennsylvania  
Philadelphia, Pennsylvania 19104

Dr. John Fontanella  
~~Department of Physics~~  
~~U.S. Naval Academy~~  
~~Annapolis, Maryland 21402-5062~~

Dr. Micha Tomkiewicz  
Department of Physics  
Brooklyn College  
Brooklyn, New York 11210

Dr. Lesser Blum  
Department of Physics  
University of Puerto Rico  
Rio Piedras, Puerto Rico 00931

Dr. Joseph Gordon, II  
IBM Corporation  
5600 Cottle Road  
San Jose, California 95193

Dr. Joel Harris  
Department of Chemistry  
University of Utah  
Salt Lake City, Utah 84112

Dr. J. O. Thomas  
University of Uppsala  
Institute of Chemistry  
Box 531 Baltimore, Maryland 21218  
S-751 21 Uppsala, Sweden

Dr. John Owen  
Department of Chemistry and  
Applied Chemistry  
University of Salford  
Salford M5 4WT UNITED KINGDOM

Dr. O. Staffsudd  
Department of Electrical Engineering  
University of California  
Los Angeles, California 90024

Dr. Boone Owens  
Department of Chemical Engineering  
and Materials Science  
University of Minnesota  
Minneapolis, Minnesota 55455

Dr. Johann A. Joebstl  
USA Mobility Equipment R&D Command  
DRDME-EC  
Fort Belvoir, Virginia 22060

Dr. Albert R. Landgrebe  
U.S. Department of Energy  
M.S. 6B025 Forrestal Building  
Washington, D.C. 20595

Dr. J. J. Brophy  
Department of Physics  
University of Utah  
Salt Lake City, Utah 84112

Dr. Charles Martin  
Department of Chemistry  
Texas A&M University  
College Station, Texas 77843

Dr. Milos Novotny  
Department of Chemistry  
Indiana University  
Bloomington, Indiana 47405

Dr. Mark A. McHugh  
Department of Chemical Engineering  
The Johns Hopkins University  
Baltimore, Maryland 21218

Dr. D. E. Irish  
Department of Chemistry  
University of Waterloo  
Waterloo, Ontario, Canada  
N2L 3G1

DL/1113/87/2

ABSTRACTS DISTRIBUTION LIST, 359/627

Dr. Henry S. White  
Department of Chemical Engineering  
and Materials Science  
151 Amundson Hall  
421 Washington Avenue, S.E.  
Minneapolis, Minnesota 55455

Dr. Daniel A. Buttry  
Department of Chemistry  
University of Wyoming  
Laramie, Wyoming 82071

Dr. W. R. Fawcett  
Department of Chemistry  
University of California  
Davis, California 95616

Dr. Peter M. Blonsky  
Eveready Battery Company, Inc.  
25225 Detroit Road, P.O. Box 45035  
Westlake, Ohio 44145

END

9-87

DTIC